Acta Cryst E
CRYSTALLOGRAPHIC COMMUNICATIONS

ISSN 2056-9890

Syntheses and structures of spontaneously resolved (2*S*)-2-phenyl-3-(thiazol-2-yl)-2,3,5,6-tetrahydro-4*H*-1,3-thiazin-4-one and racemic 2-(furan-2-yl)-3-phenyl-2,3,5,6-tetrahydro-4*H*-1,3-thiazin-4-one

Hemant P. Yennawar,[a] Tapas K. Mal,[b] Mark A. Olsen,[c] Anthony F. Lagalante,[c] Aloura D. Gavalis,[d] Isabella G. Frederick,[d] Evelyn M. Louca[d] and Lee J. Silverberg[d]*

[a]Department of Biochemistry and Molecular Biology, The Pennsylvania State University, University Park, PA 16802, USA, [b]Department of Chemistry, The Pennsylvania State University, University Park, PA 16802, USA, [c]Mendel Science Center, Villanova University, 800 Lancaster Avenue, Villanova, PA 19085, USA, and [d]Pennsylvania State University, Schuylkill Campus, 200 University Drive, Schuylkill Haven, PA 17972, USA. *Correspondence e-mail: ljs43@psu.edu

Received 10 October 2025
Accepted 20 October 2025

Edited by W. T. A. Harrison, University of Aberdeen, United Kingdom

Keywords: crystal structure; spontaneous resolution; half-chair; thiazine ring pucker.

CCDC references: 2496686; 2496685

Supporting information: this article has supporting information at journals.iucr.org/e

The title compounds, one a thiazole derivative: (2*S*)-2-phenyl-3-(thiazol-2-yl)-2,3,5,6-tetrahydro-4*H*-1,3-thiazin-4-one, $C_{13}H_{12}N_2OS_2$, and the second a furan derivative: (*rac*)-2-(furan-2-yl)-3-phenyl-2,3,5,6-tetrahydro-4*H*-1,3-thiazin-4-one, $C_{14}H_{13}NO_2S$, crystallize in space-groups $P2_12_12_1$ and $P2_1/c$, respectively, with a single molecule in their asymmetric units. The crystal of the thiazole derivative chosen for data collection was found to consist of the *S* enantiomer [Flack parameter 0.013 (9)]. The crystal of the furan derivative in the centrosymmetric space group is a racemic mixture. The puckering of the thiazine ring in both the structures is a half-chair. The extended structure of the thiazole derivative shows two weak C—H⋯O type interactions, but no aromatic ring interactions. In the structure of the furan derivative, an extensive and continuous network of C—H⋯O hydrogen bonds between the furan and the substituted thiazine ring, and also between symmetry-related furan rings, results in a continuous amphiphilic layer lying parallel to the (100) plane. Adjacent to this plane is the layer of hydrophobic phenyl rings. Thus, the extended structure comprises alternating layers of amphiphilic and hydrophobic regions, stacked in the *a*-axis direction. A C—H⋯O interaction between the phenyl ring and the thiazin-4-one moiety and the π–π stacking of the phenyl rings between pairs of symmetry-related molecules further consolidates the extended structure.

1. Chemical context

Compounds with a 2,3-diaryl-2,3,5,6-tetrahydro-4*H*-1,3-thiazin-4-one scaffold have been shown to have a variety of bioactivities, including antiparasite (Malfara *et al.*, 2021), antitumor (Chen *et al.*, 2012; Dandia *et al.*, 2013), antifungal (Ten Haken & Beatrice, 1983; Qu *et al.*, 2013.; Dandia *et al.*, 2004; Krumkains, 1984), antitubercular (Dandia *et al.*, 2004), antidiabetic (Arya *et al.*, 2012), inhibition of cannabinoid receptor 1 (CB1) (Choi *et al.*, 2008), inhibition of angiogenesis (possible treatment of eye disease, neoplasm, arteriosclerosis, arthritis, psoriasis, diabetes, and mellitus) (Yi *et al.*, 2012), regulation of plant growth (Krumkains, 1984), antimicrobial (Mogilaiah *et al.*, 1999) and antibacterial (Mahdi & Rasheed, 2023) effects.

We have previously used our T3P method to synthesize two series of these compounds in which the aryl rings on positions 2 and 3 had a variety of substituents on them (Silverberg *et al.*, 2020, 2025). Currently, another series in which one of the aryl rings is a heteroaryl is being synthesized. Here we report the syntheses and crystal structures of two new compounds in this

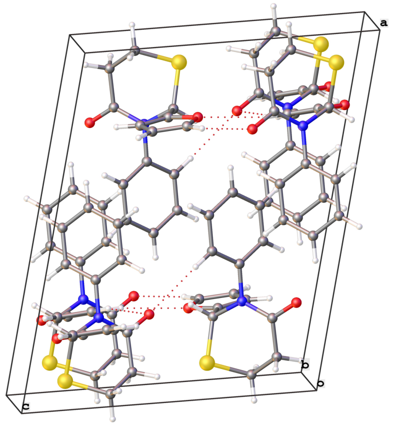

series, one in which there is a thiazole ring attached to N3 (compound **1**) and one in which there is a furan ring on C2 (compound **2**). Thiazole and furan derivatives are each known for their biological activity (Niu *et al.*, 2023; Nivrutti, 2024) and could have interesting effects on the activity of the 2,3,5,6-tetrahydro-4*H*-1,3-thiazin-4-ones.

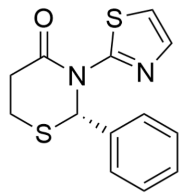

1

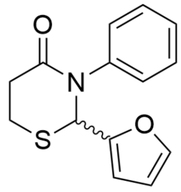

2

The spontaneous resolution of a racemic solution by direct crystallization to form a conglomerate, a mechanical mixture of separate homochiral crystals, is an uncommon but well-known phenomenon, recognized first by Pasteur (Pasteur, 1848; Jacques *et al.*, 1981; Eliel & Wilen, 1994; Pérez-García & Amabilino, 2007). It has even been used in the production of chiral active pharmaceutical ingredients (Bredikhin & Bredikhina, 2017). However, the reasons why this occurs with a minority of molecules are not well understood (Pérez-García & Amabilino, 2007) and have not yet yielded to attempts to predict occurrence (D'Oria *et al.*, 2010; Pérez-García & Amabilino, 2007).

2. Structural commentary

Compounds **1** (Fig. 1) and **2** (Fig. 2) crystallize in the orthorhombic $P2_12_12_1$ and monoclinic $P2_1/c$ space groups, respectively, with a single molecule in the respective asymmetric units. The chosen crystal of **1** was found to be composed of molecules with an *S* configuration at the stereogenic atom C1 [Flack parameter 0.013 (9)]. We had previously observed a similar spontaneous resolution in another thiazine compound (Yennawar, Bradley *et al.*, 2018). The crystal of **2** belongs to a centrosymmetric space group and must be a racemic mixture of molecules.

The thiazine rings of **1** and **2** both display a half-chair (pucker) conformation [Q = 0.694 (2), 0.6482 (11) Å; θ = 47.75 (17), 47.02 (10)°; φ = 347.4 (3), 349.01 (16)°, respectively] where the sulfur atom forms the back of the chair. We have observed this mode of puckering earlier (Yennawar, Yang *et al.*, 2016; Yennawar, Fox *et al.*, 2016; Yennawar, Bradley *et al.*, 2018), which is different from the screw-boat (Yennawar, Bendinsky *et al.*, 2014; Yennawar, Fox *et al.*, 2017; Yennawar, Noble *et al.*, 2017; Yennawar, Mal *et al.*, 2023) conformation or the envelope pucker (Yennawar, Singh *et al.*, 2014).

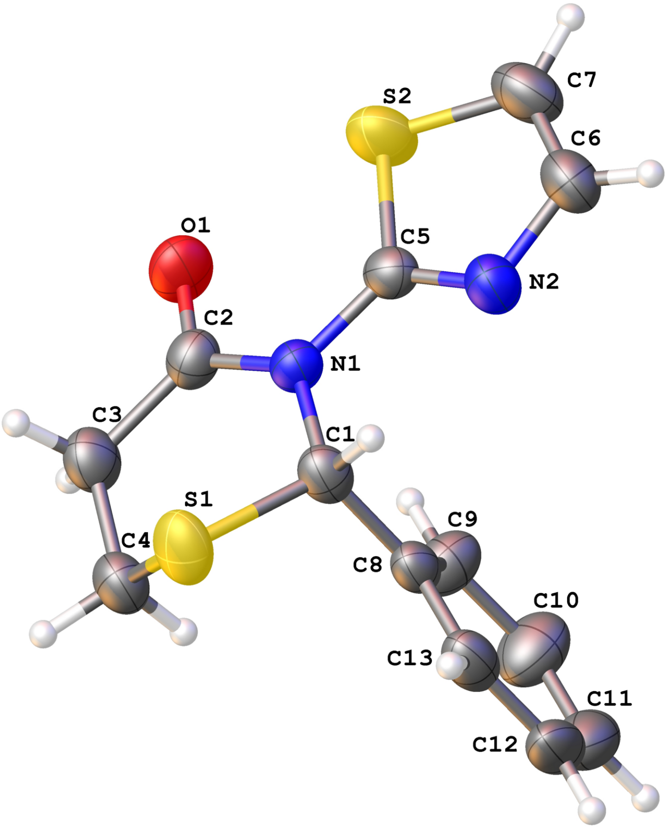

Figure 1
The molecular structure of **1** with displacement ellipsoids drawn at the 50% probability level.

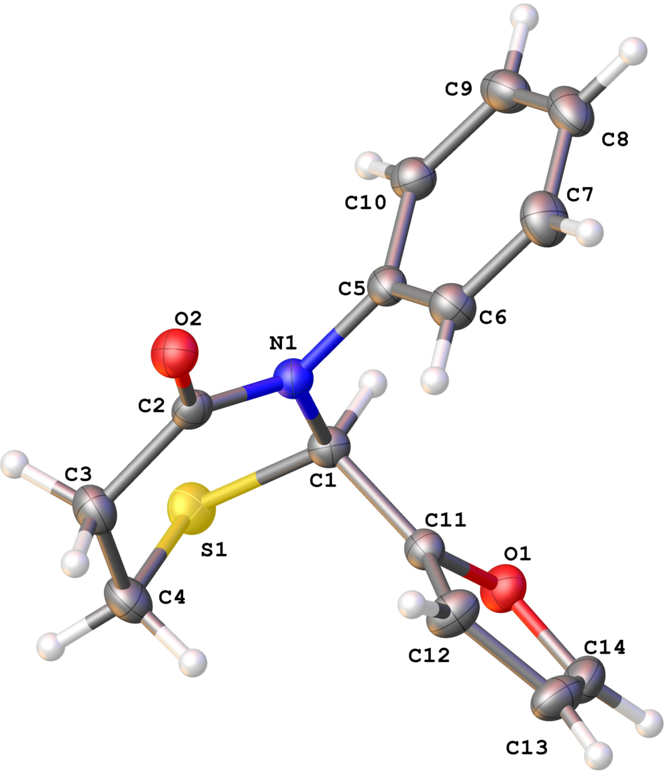

Figure 2
The molecular structure of **2** with displacement ellipsoids drawn at the 50% probability level.

Table 1
Hydrogen-bond geometry (Å, °) for **1**.

D—H⋯A	D—H	H⋯A	D⋯A	D—H⋯A
C3—H3B⋯N2^{i}	0.99	2.53	3.503 (4)	169
C7—H7⋯O1^{ii}	0.95	2.62	3.495 (3)	154

Symmetry codes: (i) $x-\frac{1}{2}, -y+\frac{3}{2}, -z+1$; (ii) $-x+\frac{3}{2}, -y+2, z-\frac{1}{2}$.

In the structure of **1**, the C5/C6/C7/N2/S2 thiazole ring and the five non-S atoms of the thiazine ring are almost coplanar, while the dihedral angle between the thiazole and the C8–C13 phenyl ring is 81.91 (13)°. In **2**, the C5–C10 phenyl and C11–C14/O1 furan rings flip positions as compared to the phenyl and thiazole rings in **1.** The phenyl ring is *gauche* with respect to the plane of the thiazine ring's five non-S atoms. The dihedral angle between the phenyl and furan ring planes is 88.45 (7)°.

3. Supramolecular features

The extended structure of **1** (Table 1, Fig. 3) features C7—H7⋯O1 hydrogen bonds forming molecular chains along the *c*-axis direction and C3—H3B⋯N2 hydrogen bonds forming chains along the *a*-axis direction. No π–π stacking interactions or layering of any kind is observed in the extended structure. The crystal of **2** on the other hand (Fig. 4) is brought about by a continuous and extensive network of intermolecular hydrogen bonds (Table 2). These include the oxygen atom on the substituted thiazine ring acting as a double acceptor for the C13—H13⋯O2 and C14—H14⋯O2 bonds and also between symmetry-related furan rings (C12—H12⋯O1). These interactions result in infinite layers of furan and thiazine moieties lying parallel to the (100) plane. Additional interaction between a carbon atom of the phenyl ring and the oxygen atom on the thiazine ring (C10—H10⋯O2) and the π–π stacking of the phenyl rings between pairs of molecules further consolidate the packing. Alternating layers of amphiphilic (furan and thiazine) and hydrophobic (phenyl) entities, parallel to the (100) plane are a feature of this structure.

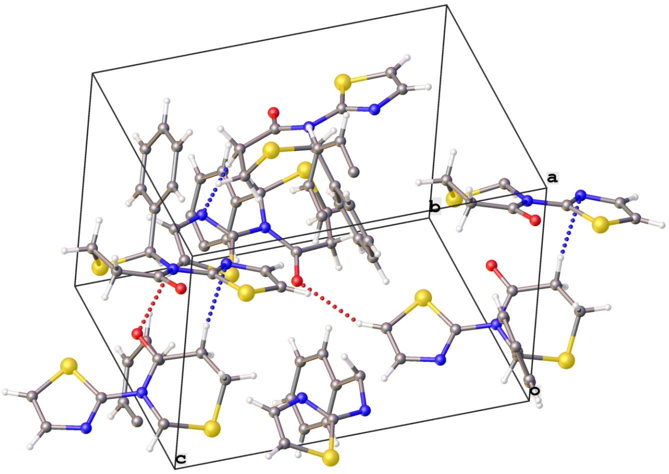

Figure 3
Crystal packing diagram of **1** with red dotted lines for C—H⋯O contacts and blue dotted lines for the C—H⋯N contacts.

Table 2
Hydrogen-bond geometry (Å, °) for **2**.

D—H⋯A	D—H	H⋯A	D⋯A	D—H⋯A
C10—H10⋯O2^{i}	0.95	2.54	3.4276 (16)	155
C12—H12⋯O1^{ii}	0.95	2.58	3.4583 (16)	153
C14—H14⋯O2^{iii}	0.95	2.50	3.4252 (16)	166
C13—H13⋯O2^{iv}	0.95	2.43	3.3641 (16)	168

Symmetry codes: (i) $x, -y+\frac{1}{2}, z+\frac{1}{2}$; (ii) $x, -y+\frac{3}{2}, z-\frac{1}{2}$; (iii) $x, -y+\frac{3}{2}, z+\frac{1}{2}$; (iv) $x, y+1, z$.

4. Database survey

We have previously reported the crystal structures of 2,3-diphenyl-2,3,5,6-tetrahydro-4*H*-1,3-thiazin-4-one (Yennawar & Silverberg, 2014, 2015), *N*-[(2*S*,5*R*)-4-oxo-2,3-diphenyl-1,3-thiazinan-5-yl] acetamide 0.375 hydrate (Yennawar *et al.*, 2015), (2*S*)-2-(3-nitrophenyl)-3-phenyl-2,3,5,6-tetrahydro-4*H*-1,3-thiazin-4-one (Yennawar, Bradley *et al.*, 2018), *rac*-2-(4-nitrophenyl)-3-phenyl-2,3,5,6-tetrahydro-4*H*-1,3-thiazin-4-one (Yennawar, Bradley *et al.*, 2018), racemic (*R**,*R**)-2,2′-(1,4-phenylene)bis(3-phenyl-2,3,5,6-tetrahydro-4*H*-1,3-thiazin-4-one) (Yennawar *et al.*, 2021), and *meso*-3,3′-(1,4-phenylene)bis(2-phenyl-2,3,5,6-tetrahydro-4*H*-1,3-thiazin-4-one) (Yennawar, Moyer & Silverberg, 2018). A literature

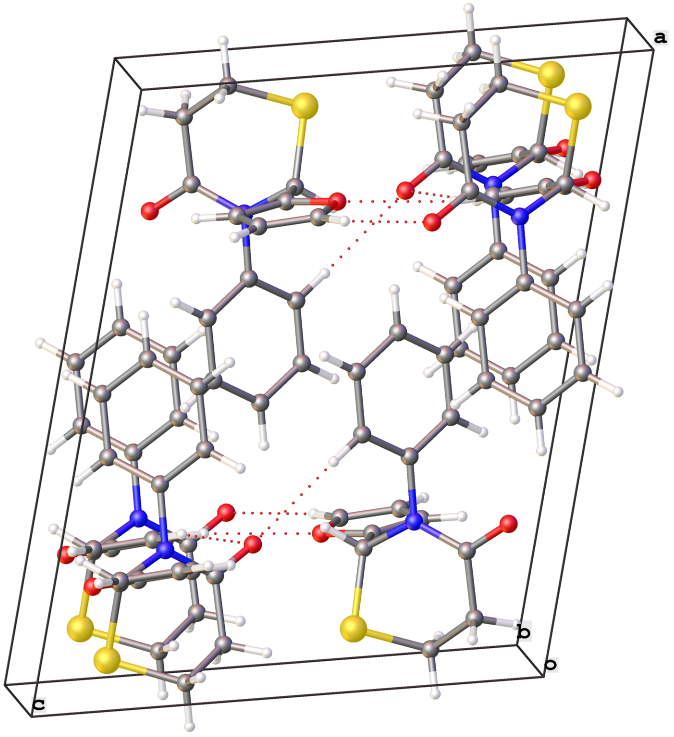

Figure 4
Crystal packing diagram of **2** showing alternating layers of amphiphilic and hydrophobic regions. Red dotted lines represent the C—H⋯O contacts.

Table 3
Experimental details.

	1	2
Crystal data		
Chemical formula	$C_{13}H_{12}N_2OS_2$	$C_{14}H_{13}NO_2S$
M_r	276.37	259.31
Crystal system, space group	Orthorhombic, $P2_12_12_1$	Monoclinic, $P2_1/c$
Temperature (K)	173	173
a, b, c (Å)	9.71506 (15), 10.04091 (13), 13.06169 (18)	14.0188 (2), 8.0422 (1), 11.3223 (2)
α, β, γ (°)	90, 90, 90	90, 104.066 (1), 90
V (Å^3)	1274.14 (3)	1238.22 (3)
Z	4	4
Radiation type	Cu $K\alpha$	Cu $K\alpha$
μ (mm^{-1})	3.69	2.27
Crystal size (mm)	0.15 × 0.10 × 0.05	0.19 × 0.18 × 0.09
Data collection		
Diffractometer	ROD, SynergyCustom system, HyPix-Arc 150	ROD, SynergyCustom system, HyPix-Arc 150
Absorption correction	Multi-scan (*CrysAlis PRO*; Rigaku OD, 2025)	Multi-scan (*CrysAlis PRO*; Rigaku OD, 2025)
$T_{\min}$, $T_{\max}$	0.820, 1.000	0.813, 1.000
No. of measured, independent and observed [$I > 2\sigma(I)$] reflections	15582, 2577, 2456	7838, 2435, 2322
$R_{\rm int}$	0.037	0.021
(sin $\theta/\lambda)_{\max}$ (Å^{-1})	0.631	0.630
Refinement		
$R[F^2 > 2\sigma(F^2)]$, $wR(F^2)$, S	0.028, 0.073, 1.05	0.029, 0.080, 1.08
No. of reflections	2577	2435
No. of parameters	164	164
H-atom treatment	H-atom parameters constrained	H-atom parameters constrained
$\Delta\rho_{\max}$, $\Delta\rho_{\min}$ (e Å^{-3})	0.14, −0.18	0.28, −0.30
Absolute structure	Flack x determined using 979 quotients $[(I^+)-(I^-)]/[(I^+)+(I^-)]$ (Parsons *et al.*, 2013)	–
Absolute structure parameter	0.013 (9)	–

Computer programs: *CrysAlis PRO* (Rigaku OD, 2025), *SHELXT* (Sheldrick, 2015*a*), *SHELXL2018/3* (Sheldrick, 2015*b*) and *OLEX2* (Dolomanov *et al.*, 2009).

survey did not reveal crystal structures of any other 2,3-diaryl-2,3,5,6-tetrahydro-4*H*-1,3-thiazin-4-ones.

5. Synthesis and crystallization

TLC plates (silica gel GF, 250-micron, 10 × 20 cm, cat. No. P21521) were purchased from Miles Scientific. TLCs were visualized under short wave UV, and then with I_2, and then by spraying with ceric ammonium nitrate/sulfuric acid and heating. Infrared spectra were run on a Thermo-Fisher NICOLET iS50 FT-IR using a diamond-ATR attachment for direct powder analysis (Penn State Schuylkill). ^{1}H and ^{13}C NMR experiments (Penn State's shared NMR facility, University Park) were carried out on a Bruker Avance-III-HD 500.20-MHz (1H frequency) instrument using a 5 mm Prodigy (liquid nitrogen cooled) BBOBB-1H/19F/D Z-GRD cryoprobe. Samples were dissolved in pyridine-*d*5 and analyzed at RT. Typical conditions for ^{1}H acquisition were 1 s relaxation delay, the acquisition time of 3.28 s, the spectral width of 10 kHz, 32 scans. Spectra were zero-filled to 128k points, and multiplied by exponential multiplication (EM with LB = 0.3 Hz) prior to FT. For ^{13}C experiments, data were acquired with power-gated ^{1}H decoupling using a 2 s relaxation delay, with an acquisition time of 1.1 s, spectral width of 29.8 kHz, and 256 scans. Spectra were zero-filled once, and multiplied by EM with LB = 2 Hz prior to FT. MS samples were analyzed for accurate mass by LCMS on a SCIEX Exion LC with a SCIEX 5600+ TripleTOF MS. Separation was achieved on an Agilent Infinity LabPoroshell column 120 EC-C18, 2.1 X 50mm, 2.7-micron particle (p/n 699775-902), column maintained at 313 K. Elution using a reversed phase gradient of 100% (water with 0.1% formic acid) ramped to 100% (acetonitrile with 0.1% formic acid) over 10 min at a flowrate of 0.4 mL min^{-1}. The MS was scanned over 50–1200 Da and calibrated with the SCIEX APCI positive calibrant solution (Part 4460131) prior to sample analysis. Samples were analyzed in ESI positive mode with a DP = 100 V, CE = 10, GAS1 = GAS2 = 60 psi, curtain = 30 psi, ISV = 5500 V, and source temperature of 773 K (Villanova University). Melting points were performed on a Vernier Melt Station (Penn State Schuylkill). Suitable crystals were selected and sequentially mounted using a nylon loop and a dab of paratone oil.

2-Phenyl-3-(thiazol-2-yl)-2,3,5,6-tetrahydro-4*H*-1,3-thiazin-4-one, 1: A two-necked 25 ml round-bottom flask was oven-dried, cooled under N_2, and charged with a stir bar. 2-Aminothiazole (0.6005 g, 6.00 mmol) and benzaldehyde (0.6369 g, 6.00 mmol) were added. 2-Methyltetrahydrofuran (2.3 ml) was added and the solution was stirred for five minutes. 3-Mercaptopropionic acid (0.6379 g, 6.00 mmol) was added followed by pyridine (2.9 ml, 36 mmol). Finally, 2,4,6-tripropyl-1,3,5,2,4,6-trioxatriphosphorinane-2,4,6-trioxide (T3P) in 2-methyltetrahydrofuran (50 weight percent; 11 ml, 18 mmol) was added. The reaction was stirred at room temperature and followed by TLC, then poured into a separatory funnel with dichloromethane (20 ml). The mixture was washed with water (10 ml). The aqueous was then extracted twice with dichloromethane (10 ml each). The organics were combined and washed with saturated sodium bicarbonate (10 ml) and then saturated sodium chloride (10 ml). The organic extract was dried over sodium sulfate and concentrated under vacuum to give a crude mixture. After chromatography on 30 g silica gel with mixtures of ethyl acetate and hexanes (gradient from 30% ethyl acetate to 70%), recrystallization from methanol solution gave an off-white solid (0.1186 g, 7% yield). m.p.: 426–427 K. Colorless blocks of **1** for crystallography were grown by slow evaporation from methanol solution. ^{1}H NMR (*d*5-pyridine) δ 7.65 (*s*, 1H), 7.47 (*d*, J = 3.7 Hz, 1H), 7.39 (*d*, J = 7.8 Hz, 2H), 7.26 (*t*, J = 7.6 Hz, 2H), 7.21 (*d*, J = 7.2 Hz, 1H), 7.12 (*d*, J = 3.7 Hz, 1H), 3.16–2.93 (*m*, 2H), 2.83–2.73 (*m*, 1H), 2.65–2.55 (*m*, 1H). ^{13}C NMR (d5-pyridine) δ 168.5, 158.4, 140.1, 137.4, 128.7, 127.8, 126.4, 115.9, 61.7, 34.4, 20.8. HRMS (*m*/*z*): [M + H$^+$] of 277.0465 is consistent with calculated [M + H]$^+$ of 277.0464. IR (neat, cm^{-1}): 1647 (C═O).

2-(Furan-2-yl)-3-phenyl-2,3,5,6-tetrahydro-4*H*-1,3-thiazin-4-one, 2: A two-necked 25 ml round-bottom flask was oven-dried, cooled under N_2, and charged with a stir bar. Aniline (0.5585 g, 6.00 mmol) and furfural (0.5764 g, 6.00 mmol) were added. 2-Methyltetrahydrofuran (2.3 ml) was added and the solution was stirred for five minutes. Pyridine (2.9 ml, 36 mmol) and 2,4,6-tripropyl-1,3,5,2,4,6-trioxatriphosphorinane-2,4,6-trioxide (T3P) in 2-methyltetrahydrofuran (50 weight percent; 11 ml, 18 mmol) were added. Lastly, 3-mercaptopropionic acid (0.52 ml, 6.00 mmol) was added dropwise. The reaction was stirred at room temperature and followed by TLC, then poured into a separatory funnel with ethyl acetate (20 ml). The mixture was washed with water (10 ml). The aqueous layer was then extracted twice with ethyl acetate (10 ml each). The organics were combined and washed with saturated sodium bicarbonate (10 ml) and then saturated sodium chloride (10 ml). The organic extract was dried over sodium sulfate and concentrated under vacuum to give a crude mixture. After chromatography on 30 g silica gel with mixtures of ethyl acetate and hexanes (gradient from 30% ethyl acetate to 70%), recrystallization from ethanol gave a light orange solid (0.538 g, 35% yield). m.p.: 380.1–380.9 K (decomposition). Yellow blocks of **2** were grown by slow evaporation from ethanol solution. ^{1}H NMR (*d*5-pyridine) δ 7.43 (d, J = 8.2 Hz, 2H), 7.30 (*t*, J = 7.9 Hz, 2H), 7.18 (*d*, J = 14.9 Hz, 2H), 6.49 (*d*, J = 3.4 Hz, 1H), 6.38 (*dd*, J = 3.3, 1.8 Hz, 1H), 6.32 (*s*, 1H), 3.23–3.13 (*m*, 1H), 3.07–2.92 (*m*, 2H), 2.88–2.79 (*m*, 1H). ^{13}C NMR (*d*5-pyridine) δ 168.7, 152.1, 143.2, 143.1, 129.1, 127.6, 127.2, 110.8, 109.1, 59.7, 34.7, 23.3. HRMS (*m*/*z*): [M + H$^+$] of 260.0737 is consistent with calculated [M + H]$^+$ of 260.0739. IR (neat, cm^{-1}): 1623 (C═O).

6. Refinement

Crystal data, data collection and structure refinement details are summarized in Table 3. The H atoms were placed geometrically and allowed to ride on their parent C atoms during refinement, with C—H distances of 0.95 Å (aromatic), 0.97 Å (methylene) and 1.0 Å (methyne) and with $U_{\rm iso}$(H) = 1.2$U_{\rm eq}$ (aromatic or methylene C) or 1.5$U_{\rm eq}$ (methyl C).

Acknowledgements

This work was supported by a Major Research Instrumentation Grant from the National Science Foundation to Villanova University (CHE-1827930) for the mass spectrometer; NIH S10 grants (1S10-OD028589 and 1S10-RR023439) to Dr Neela Yennawar (PSU, University Park) for the X-ray diffractometer; and by a research development grant at Penn State Schuylkill.

Funding information

Funding for this research was provided by: National Science Foundation, Directorate for Mathematical and Physical Sciences (grant No. CHE-1827930 to Villanova University); National Institutes of Health (grant No. 1S10-OD028589 to Neela Yennawar; grant No. 1S10-RR023439 to Neela Yennawar); Penn State Schuylkill (grant to Lee J. Silverberg).

References

Arya, K., Rawat, D. S., Dandia, A. & Sasai, H. (2012). *J. Fluor. Chem.* **137**, 117–122.

Bredikhin, A. A. & Bredikhina, Z. A. (2017). *Chem. Eng. & Technol.* **40**, 1211–1220.

Chen, Y., Wu, J., Yu, L., Zhai, D., Yi, Z., Luo, J. & Liu, M. (2012). CN 102653526 A.

Choi, H., Wang, Z., Zhu, X., He, X., Yang, K. & Liu, H. (2008). WO 2008112674 A1.

Dandia, A., Singh, R. & Arya, K. (2004). *Phosphorus Sulfur Silicon* **179**, 551–564.

Dandia, A., Singh, R. & Saini, D. (2013). *J. Chem. Sci.* **125**, 1045–1053.

Dolomanov, O. V., Bourhis, L. J., Gildea, R. J., Howard, J. A. K. & Puschmann, H. (2009). *J. Appl. Cryst.* **42**, 339–341.

D'Oria, E., Karamertzanis, P. G. & Price, S. L. (2010). *Cryst. Growth Des.* **10**, 1749–1756.

Eliel, E. & Wilen, S. H. (1994). *Stereochemistry of Organic Compounds.* New York: John Wiley & Sons.

Jacques, J., Collet, A. & Wilen, S. H. (1981). *Enantiomers, Racemates, and Resolutions.* New York: John Wiley & Sons.

Krumkains, E. V. (1984). EP 10420 B1.

Mahdi, H. T. & Rasheed, M. K. (2023). *J. New Mater. Electrochem. Syst.* **26**, 227–231.

Malfara, M. F., Silverberg, L. J., DiMaio, J., Lagalante, A. F., Olsen, M. A., Madison, E. & Povelones, M. L. (2021). *Mol. Biochem. Parasitol.* **245**, Article 111396.

Mogilaiah, K., Reddy, P. R. & Rao, R. B. (1999). *Ind. J. Chem.* **38B**, 495–500.

Niu, Z.-X., Wang, Y.-T., Zhang, S.-N., Li, Y., Chen, X.-B., Wang, S.-Q. & Liu, H.-M. (2023). *Eur. J. Med. Chem.* **250**, 115172.

Nivrutti, G. P. (2024). *Int. J. Adv. Biol. Biomed. Res.* **12**, 167–181.

Parsons, S., Flack, H. D. & Wagner, T. (2013). *Acta Cryst.* B**69**, 249–259.

Pasteur, L. (1848). *Ann. Chim. Phys.* **22**, 442–459.

Pérez-García, L. & Amabilino, D. B. (2007). *Chem. Soc. Rev.* **36**, 941–967.

Rigaku OD (2025). *CrysAlis PRO*. Rigaku Oxford Diffraction, Yarnton, England.

Qu, H., Zhang, R., Hu, Y., Ke, Y., Gao, Z. & Xu, H. (2013). *Z. Naturforsch. C: J. Biosci.* **68**, 77–81.

Sheldrick, G. M. (2015*a*). *Acta Cryst.* A**71**, 3–8.

Sheldrick, G. M. (2015*b*). *Acta Cryst.* C**71**, 3–8.

Silverberg, L. J., Mal, T., Lagalante, A., Olsen, M., Fleming, M., Garcia, T., Gavalis, A., Gonzalez, K., Gregory, C., Hackenberg, L., Lawler, M., Li, E., Louca, E., Mack, S., Perhonitch, K., Shaffer, K., Thompson, C., Tran, S., Vidal, E. & Vidal, R. (2025). *J. Heterocycl. Chem.* **62**, 338–344.

Silverberg, L. J., Pacheco, C., Sahu, D., Mal, T., Scholl, P., Sobhi, H. F., Bradley, H. G., Cardenas, O. A., Gonzalez, K. M., Islam, J. M., Kimmel, E. G., Li, W., Perhonitch, K. C., Pothering, J. T., Potts, M. E., Ramirez, M. E., Reppert, H. E. & Shaffer, K. N. (2020). *Tetrahedron Lett.* **61**, 151836.

Ten Haken, T. & Beatrice, S. (1983). EP 009114B1.

Yennawar, H. P., Bendinsky, R. V., Coyle, D. J., Cali, A. S. & Silverberg, L. J. (2014). *Acta Cryst.* E**70**, o465.

Yennawar, H. P., Bradley, H. G., Perhonitch, K. C., Reppert, H. E. & Silverberg, L. J. (2018). *Acta Cryst.* E**74**, 454–457.

Yennawar, H. P., Fox, R., Moyer, Q. J., Yang, Z. & Silverberg, L. J. (2017). *Acta Cryst.* E**73**, 1189–1191.

Yennawar, H. P., Fox, R. & Silverberg, L. J. (2016). *Acta Cryst.* E**72**, 276–279.

Yennawar, H. P., Mal, T. K., Pacheco, C. N., Lagalante, A. F., Olsen, M. A., Russell, M. W., Muench, G. C., Moyer, Q. J. & Silverberg, L. J. (2023). *Acta Cryst.* E**79**, 221–225.

Yennawar, H. P., Medica, J. J. & Silverberg, L. J. (2021). *Acta Cryst.* E**77**, 1263–1266.

Yennawar, H. P., Moyer, Q. J. & Silverberg, L. J. (2018). *Acta Cryst.* E**74**, 1497–1499.

Yennawar, H. P., Noble, D. J., Yang, Z. & Silverberg, L. J. (2017). *IUCrData* **2**, x171112.

Yennawar, H. P. & Silverberg, L. J. (2014). *Acta Cryst.* E**70**, o133.

Yennawar, H. P. & Silverberg, L. J. (2015). **E71**, e5.

Yennawar, H. P., Singh, H. & Silverberg, L. J. (2014). *Acta Cryst.* E**70**, o638.

Yennawar, H. P., Singh, H. & Silverberg, L. J. (2015). *Acta Cryst.* E**71**, 62–64.

Yennawar, H. P., Yang, Z. & Silverberg, L. J. (2016). *Acta Cryst.* E**72**, 1541–1543.

Yi, Z., Tong, W., Weiguang, Z., Dong, L., Wu, J., Chen, Y. & Liu, M. (2012). CN 102786493 A.

supporting information

Acta Cryst. (2025). E**81**, 1044-1049 [https://doi.org/10.1107/S2056989025009193]

Syntheses and structures of spontaneously resolved (2*S*)-2-phenyl-3-(thiazol-2-yl)-2,3,5,6-tetrahydro-4*H*-1,3-thiazin-4-one and racemic 2-(furan-2-yl)-3-phenyl-2,3,5,6-tetrahydro-4*H*-1,3-thiazin-4-one

Hemant P. Yennawar, Tapas K. Mal, Mark A. Olsen, Anthony F. Lagalante, Aloura D. Gavalis, Isabella G. Frederick, Evelyn M. Louca and Lee J. Silverberg

Computing details

(2*S*)-2-Phenyl-3-(thiazol-2-yl)-2,3,5,6-tetrahydro-4*H*-1,3-thiazin-4-one (1)

Crystal data

$C_{13}H_{12}N_2OS_2$
$M_r = 276.37$
Orthorhombic, $P2_12_12_1$
$a = 9.71506\ (15)$ Å
$b = 10.04091\ (13)$ Å
$c = 13.06169\ (18)$ Å
$V = 1274.14\ (3)$ Å^3
$Z = 4$
$F(000) = 576$

$D_x = 1.441$ Mg m^{-3}
Cu $K\alpha$ radiation, $\lambda = 1.54184$ Å
Cell parameters from 8550 reflections
$\theta = 3.4–73.4°$
$\mu = 3.69$ mm^{-1}
$T = 173$ K
Block, colorless
0.15 × 0.10 × 0.05 mm

Data collection

ROD, SynergyCustom system, HyPix-Arc 150 diffractometer
Radiation source: Rotating-anode X-ray tube, Rigaku (Cu) X-ray Source
Mirror monochromator
Detector resolution: 10.0000 pixels mm^{-1}
ω scans
Absorption correction: multi-scan (CrysAlisPro; Rigaku OD, 2025)

$T_{min} = 0.820$, $T_{max} = 1.000$
15582 measured reflections
2577 independent reflections
2456 reflections with $I > 2\sigma(I)$
$R_{int} = 0.037$
$\theta_{max} = 76.5°$, $\theta_{min} = 5.6°$
$h = -10 \rightarrow 12$
$k = -12 \rightarrow 12$
$l = -16 \rightarrow 16$

Refinement

Refinement on F^2
Least-squares matrix: full
$R[F^2 > 2\sigma(F^2)] = 0.028$
$wR(F^2) = 0.073$
$S = 1.05$
2577 reflections
164 parameters
0 restraints
Hydrogen site location: inferred from neighbouring sites
H-atom parameters constrained

$w = 1/[\sigma^2(F_o^2) + (0.0356P)^2 + 0.1897P]$ where $P = (F_o^2 + 2F_c^2)/3$
$(\Delta/\sigma)_{max} < 0.001$
$\Delta\rho_{max} = 0.14$ e Å^{-3}
$\Delta\rho_{min} = -0.18$ e Å^{-3}
Extinction correction: SHELXL-2018/3 (Sheldrick 2015b), $Fc^* = kFc[1+0.001xFc^2\lambda^3/\sin(2\theta)]^{-1/4}$
Extinction coefficient: 0.0019 (4)

Absolute structure: Flack *x* determined using 979 quotients $[(I^+)-(I^-)]/[(I^+)+(I^-)]$ (Parsons *et al.*, 2013)
Absolute structure parameter: 0.013 (9)

Special details

Geometry. All esds (except the esd in the dihedral angle between two l.s. planes) are estimated using the full covariance matrix. The cell esds are taken into account individually in the estimation of esds in distances, angles and torsion angles; correlations between esds in cell parameters are only used when they are defined by crystal symmetry. An approximate (isotropic) treatment of cell esds is used for estimating esds involving l.s. planes.

Fractional atomic coordinates and isotropic or equivalent isotropic displacement parameters (Å²)

	x	*y*	*z*	U_{iso}*/U_{eq}
S1	0.89569 (8)	0.55653 (7)	0.61560 (5)	0.0551 (2)
S2	0.80954 (8)	0.91269 (7)	0.30808 (6)	0.0584 (2)
O1	0.7233 (2)	0.91808 (17)	0.49817 (15)	0.0560 (5)
N1	0.8157 (2)	0.71837 (18)	0.45942 (14)	0.0372 (4)
N2	0.8863 (2)	0.6695 (2)	0.29155 (16)	0.0492 (5)
C1	0.8492 (2)	0.5775 (2)	0.48283 (18)	0.0403 (5)
H1	0.932918	0.554839	0.441811	0.048*
C8	0.7369 (3)	0.4831 (2)	0.44846 (17)	0.0394 (5)
C2	0.7542 (2)	0.8056 (2)	0.52664 (19)	0.0410 (5)
C9	0.6083 (3)	0.5254 (3)	0.4168 (2)	0.0533 (7)
H9	0.586998	0.617694	0.417852	0.064*
C5	0.8384 (2)	0.7550 (2)	0.35675 (18)	0.0381 (5)
C6	0.9008 (3)	0.7284 (3)	0.1967 (2)	0.0548 (7)
H6	0.933586	0.680501	0.138953	0.066*
C13	0.7641 (4)	0.3466 (3)	0.4476 (2)	0.0536 (7)
H13	0.851329	0.314590	0.469296	0.064*
C4	0.7364 (3)	0.6209 (3)	0.6645 (2)	0.0511 (7)
H4A	0.657947	0.571637	0.634444	0.061*
H4B	0.733136	0.610383	0.739804	0.061*
C3	0.7273 (3)	0.7666 (3)	0.6364 (2)	0.0488 (6)
H3A	0.793298	0.815724	0.680090	0.059*
H3B	0.633938	0.798117	0.654775	0.059*
C12	0.6630 (5)	0.2569 (3)	0.4149 (2)	0.0687 (10)
H12	0.681842	0.164056	0.415077	0.082*
C7	0.8660 (3)	0.8566 (3)	0.1911 (2)	0.0600 (8)
H7	0.871548	0.909530	0.130911	0.072*
C10	0.5096 (3)	0.4347 (3)	0.3836 (3)	0.0681 (9)
H10	0.422186	0.465784	0.361365	0.082*
C11	0.5374 (4)	0.3017 (3)	0.3825 (3)	0.0682 (9)
H11	0.469717	0.240301	0.359493	0.082*

Atomic displacement parameters (Å²)

	U^{11}	U^{22}	U^{33}	U^{12}	U^{13}	U^{23}
S1	0.0709 (4)	0.0553 (4)	0.0391 (3)	0.0174 (3)	−0.0116 (3)	0.0017 (3)

S2	0.0820 (5)	0.0416 (4)	0.0515 (4)	0.0087 (3)	0.0069 (4)	0.0116 (3)
O1	0.0800 (13)	0.0353 (9)	0.0527 (10)	0.0115 (9)	0.0006 (9)	−0.0027 (8)
N1	0.0463 (10)	0.0299 (9)	0.0354 (10)	0.0011 (8)	0.0000 (9)	−0.0002 (8)
N2	0.0680 (14)	0.0432 (12)	0.0364 (11)	−0.0006 (11)	0.0043 (10)	−0.0001 (9)
C1	0.0505 (13)	0.0361 (12)	0.0343 (11)	0.0096 (10)	0.0023 (9)	0.0018 (10)
C8	0.0581 (14)	0.0317 (11)	0.0284 (10)	0.0009 (10)	0.0081 (10)	−0.0006 (9)
C2	0.0458 (12)	0.0363 (12)	0.0409 (12)	0.0014 (10)	−0.0022 (10)	−0.0055 (10)
C9	0.0532 (15)	0.0405 (13)	0.0660 (18)	−0.0014 (12)	0.0024 (13)	−0.0090 (12)
C5	0.0424 (11)	0.0350 (11)	0.0369 (12)	−0.0034 (9)	−0.0027 (9)	0.0022 (9)
C6	0.0694 (17)	0.0591 (17)	0.0359 (13)	−0.0055 (14)	0.0043 (13)	0.0028 (12)
C13	0.088 (2)	0.0378 (13)	0.0352 (13)	0.0093 (13)	0.0069 (13)	0.0027 (10)
C4	0.0691 (17)	0.0500 (15)	0.0341 (12)	−0.0018 (13)	0.0029 (12)	0.0007 (11)
C3	0.0583 (15)	0.0479 (14)	0.0401 (13)	0.0051 (12)	0.0069 (11)	−0.0044 (11)
C12	0.131 (3)	0.0312 (14)	0.0434 (15)	−0.0125 (17)	0.0188 (18)	−0.0030 (11)
C7	0.0734 (19)	0.0614 (18)	0.0452 (15)	−0.0007 (14)	0.0053 (14)	0.0158 (14)
C10	0.0595 (17)	0.0628 (19)	0.082 (2)	−0.0120 (15)	0.0055 (16)	−0.0157 (19)
C11	0.089 (2)	0.0566 (18)	0.0594 (18)	−0.0269 (17)	0.0190 (18)	−0.0084 (17)

Geometric parameters (Å, º)

S1—C1	1.804 (2)	C9—C10	1.392 (4)
S1—C4	1.795 (3)	C6—H6	0.9500
S2—C5	1.730 (2)	C6—C7	1.333 (4)
S2—C7	1.718 (3)	C13—H13	0.9500
O1—C2	1.226 (3)	C13—C12	1.400 (5)
N1—C1	1.484 (3)	C4—H4A	0.9900
N1—C2	1.377 (3)	C4—H4B	0.9900
N1—C5	1.408 (3)	C4—C3	1.510 (4)
N2—C5	1.295 (3)	C3—H3A	0.9900
N2—C6	1.380 (3)	C3—H3B	0.9900
C1—H1	1.0000	C12—H12	0.9500
C1—C8	1.513 (3)	C12—C11	1.368 (5)
C8—C9	1.383 (4)	C7—H7	0.9500
C8—C13	1.395 (3)	C10—H10	0.9500
C2—C3	1.510 (4)	C10—C11	1.363 (5)
C9—H9	0.9500	C11—H11	0.9500

C4—S1—C1	94.83 (12)	C8—C13—H13	119.9
C7—S2—C5	88.58 (13)	C8—C13—C12	120.1 (3)
C2—N1—C1	124.80 (19)	C12—C13—H13	119.9
C2—N1—C5	120.63 (19)	S1—C4—H4A	110.0
C5—N1—C1	114.25 (18)	S1—C4—H4B	110.0
C5—N2—C6	110.1 (2)	H4A—C4—H4B	108.4
S1—C1—H1	106.6	C3—C4—S1	108.26 (19)
N1—C1—S1	111.35 (16)	C3—C4—H4A	110.0
N1—C1—H1	106.6	C3—C4—H4B	110.0
N1—C1—C8	112.22 (19)	C2—C3—C4	118.2 (2)
C8—C1—S1	113.11 (16)	C2—C3—H3A	107.8

C8—C1—H1	106.6	C2—C3—H3B	107.8
C9—C8—C1	123.2 (2)	C4—C3—H3A	107.8
C9—C8—C13	118.0 (3)	C4—C3—H3B	107.8
C13—C8—C1	118.8 (3)	H3A—C3—H3B	107.1
O1—C2—N1	119.9 (2)	C13—C12—H12	119.7
O1—C2—C3	119.0 (2)	C11—C12—C13	120.6 (3)
N1—C2—C3	121.0 (2)	C11—C12—H12	119.7
C8—C9—H9	119.5	S2—C7—H7	124.8
C8—C9—C10	121.0 (3)	C6—C7—S2	110.4 (2)
C10—C9—H9	119.5	C6—C7—H7	124.8
N1—C5—S2	124.30 (17)	C9—C10—H10	119.7
N2—C5—S2	115.03 (17)	C11—C10—C9	120.5 (3)
N2—C5—N1	120.7 (2)	C11—C10—H10	119.7
N2—C6—H6	122.0	C12—C11—H11	120.1
C7—C6—N2	116.0 (3)	C10—C11—C12	119.7 (3)
C7—C6—H6	122.0	C10—C11—H11	120.1

S1—C1—C8—C9	115.7 (2)	C2—N1—C5—S2	6.7 (3)
S1—C1—C8—C13	−64.8 (3)	C2—N1—C5—N2	−174.5 (2)
S1—C4—C3—C2	49.7 (3)	C9—C8—C13—C12	0.4 (4)
O1—C2—C3—C4	166.8 (3)	C9—C10—C11—C12	0.2 (5)
N1—C1—C8—C9	−11.3 (3)	C5—S2—C7—C6	0.1 (2)
N1—C1—C8—C13	168.2 (2)	C5—N1—C1—S1	153.07 (17)
N1—C2—C3—C4	−14.8 (4)	C5—N1—C1—C8	−79.0 (2)
N2—C6—C7—S2	−0.5 (4)	C5—N1—C2—O1	−2.7 (4)
C1—S1—C4—C3	−65.9 (2)	C5—N1—C2—C3	179.0 (2)
C1—N1—C2—O1	−175.7 (2)	C5—N2—C6—C7	0.8 (4)
C1—N1—C2—C3	5.9 (4)	C6—N2—C5—S2	−0.7 (3)
C1—N1—C5—S2	−179.52 (17)	C6—N2—C5—N1	−179.5 (2)
C1—N1—C5—N2	−0.8 (3)	C13—C8—C9—C10	−1.0 (4)
C1—C8—C9—C10	178.4 (3)	C13—C12—C11—C10	−0.9 (5)
C1—C8—C13—C12	−179.1 (2)	C4—S1—C1—N1	58.12 (18)
C8—C9—C10—C11	0.7 (5)	C4—S1—C1—C8	−69.34 (18)
C8—C13—C12—C11	0.6 (4)	C7—S2—C5—N1	179.1 (2)
C2—N1—C1—S1	−33.5 (3)	C7—S2—C5—N2	0.3 (2)
C2—N1—C1—C8	94.5 (3)		

Hydrogen-bond geometry (Å, º)

D—H···*A*	*D*—H	H···*A*	*D*···*A*	*D*—H···*A*
C3—H3*B*···N2$^{\text{i}}$	0.99	2.53	3.503 (4)	169
C7—H7···O1$^{\text{ii}}$	0.95	2.62	3.495 (3)	154

Symmetry codes: (i) *x*−1/2, −*y*+3/2, −*z*+1; (ii) −*x*+3/2, −*y*+2, *z*−1/2.

2-(Furan-2-yl)-3-phenyl-2,3,5,6-tetrahydro-4*H*-1,3-thiazin-4-one (2)

Crystal data

$C_{14}H_{13}NO_2S$	$F(000) = 544$
$M_r = 259.31$	$D_x = 1.391$ Mg m^{-3}
Monoclinic, $P2_1/c$	Cu $K\alpha$ radiation, $\lambda = 1.54184$ Å
$a = 14.0188$ (2) Å	Cell parameters from 5692 reflections
$b = 8.0422$ (1) Å	$\theta = 3.2$–$76.2°$
$c = 11.3223$ (2) Å	$\mu = 2.27$ mm^{-1}
$\beta = 104.066$ (1)°	$T = 173$ K
$V = 1238.22$ (3) Å^3	Block, yellow
$Z = 4$	0.19 × 0.18 × 0.09 mm

Data collection

ROD, SynergyCustom system, HyPix-Arc 150 diffractometer	2435 independent reflections
Detector resolution: 10.0000 pixels mm^{-1}	2322 reflections with $I > 2\sigma(I)$
ω scans	$R_{\text{int}} = 0.021$
Absorption correction: multi-scan (CrysAlisPro; Rigaku OD, 2025)	$\theta_{\max} = 76.3°$, $\theta_{\min} = 3.3°$
$T_{\min} = 0.813$, $T_{\max} = 1.000$	$h = -17 \rightarrow 15$
7838 measured reflections	$k = -9 \rightarrow 9$
	$l = -12 \rightarrow 13$

Refinement

Refinement on F^2	H-atom parameters constrained
Least-squares matrix: full	$w = 1/[\sigma^2(F_o^2) + (0.0403P)^2 + 0.4195P]$ where $P = (F_o^2 + 2F_c^2)/3$
$R[F^2 > 2\sigma(F^2)] = 0.029$	$(\Delta/\sigma)_{\max} < 0.001$
$wR(F^2) = 0.080$	$\Delta\rho_{\max} = 0.28$ e Å^{-3}
$S = 1.08$	$\Delta\rho_{\min} = -0.30$ e Å^{-3}
2435 reflections	Extinction correction: SHELXL-2018/3 (Sheldrick 2015b), $Fc^* = kFc[1+0.001xFc^2\lambda^3/\sin(2\theta)]^{-1/4}$
164 parameters	Extinction coefficient: 0.0077 (5)
0 restraints	
Hydrogen site location: inferred from neighbouring sites	

Special details

Geometry. All esds (except the esd in the dihedral angle between two l.s. planes) are estimated using the full covariance matrix. The cell esds are taken into account individually in the estimation of esds in distances, angles and torsion angles; correlations between esds in cell parameters are only used when they are defined by crystal symmetry. An approximate (isotropic) treatment of cell esds is used for estimating esds involving l.s. planes.

Fractional atomic coordinates and isotropic or equivalent isotropic displacement parameters (Å^2)

	x	*y*	*z*	U_{iso}*/U_{eq}
S1	0.07806 (2)	0.43110 (4)	0.36542 (3)	0.02744 (13)
O2	0.23770 (7)	0.25789 (11)	0.10605 (8)	0.0256 (2)
O1	0.21764 (7)	0.77273 (11)	0.44109 (8)	0.0254 (2)
N1	0.24650 (7)	0.38603 (13)	0.28567 (9)	0.0190 (2)
C11	0.21704 (8)	0.66614 (15)	0.34668 (10)	0.0194 (3)
C5	0.35291 (8)	0.37345 (15)	0.31819 (11)	0.0202 (3)
C4	0.19546 (9)	0.32966 (15)	0.17485 (11)	0.0200 (3)
C1	0.20443 (8)	0.48549 (15)	0.37027 (10)	0.0196 (3)
H1	0.244178	0.461383	0.454540	0.024*

C10	0.39909 (9)	0.29220 (16)	0.42481 (11)	0.0240 (3)
H10	0.361323	0.242939	0.474755	0.029*
C12	0.22949 (10)	0.75125 (16)	0.24929 (12)	0.0272 (3)
H12	0.231244	0.706306	0.172252	0.033*
C6	0.40772 (9)	0.44727 (16)	0.24559 (12)	0.0254 (3)
H6	0.375659	0.503820	0.173134	0.030*
C14	0.23214 (10)	0.92929 (16)	0.39920 (13)	0.0288 (3)
H14	0.236273	1.028377	0.445845	0.035*
C3	0.08435 (9)	0.34646 (18)	0.13502 (12)	0.0280 (3)
H3A	0.067243	0.381193	0.048541	0.034*
H3B	0.055757	0.234554	0.138570	0.034*
C9	0.50141 (10)	0.28352 (17)	0.45798 (12)	0.0293 (3)
H9	0.533662	0.227828	0.530735	0.035*
C8	0.55618 (9)	0.35590 (18)	0.38510 (13)	0.0310 (3)
H8	0.625913	0.349154	0.407707	0.037*
C7	0.50956 (10)	0.43809 (18)	0.27934 (13)	0.0305 (3)
H7	0.547376	0.488261	0.229822	0.037*
C2	0.03348 (9)	0.46475 (18)	0.20431 (12)	0.0297 (3)
H2A	−0.038455	0.446094	0.180119	0.036*
H2B	0.046518	0.581040	0.184200	0.036*
C13	0.23958 (10)	0.92243 (16)	0.28411 (14)	0.0299 (3)
H13	0.249607	1.013374	0.234946	0.036*

Atomic displacement parameters (Å^2)

	U^{11}	U^{22}	U^{33}	U^{12}	U^{13}	U^{23}
S1	0.02374 (18)	0.0304 (2)	0.0316 (2)	−0.00259 (12)	0.01330 (13)	0.00038 (12)
O2	0.0287 (5)	0.0262 (5)	0.0225 (5)	0.0000 (4)	0.0073 (3)	−0.0041 (4)
O1	0.0306 (5)	0.0235 (5)	0.0217 (5)	−0.0001 (4)	0.0056 (3)	−0.0048 (3)
N1	0.0185 (5)	0.0189 (5)	0.0200 (5)	0.0004 (4)	0.0053 (4)	−0.0012 (4)
C11	0.0191 (5)	0.0204 (6)	0.0188 (6)	0.0008 (4)	0.0045 (4)	−0.0031 (4)
C5	0.0195 (6)	0.0183 (6)	0.0223 (6)	0.0006 (4)	0.0042 (4)	−0.0036 (5)
C4	0.0233 (6)	0.0162 (5)	0.0200 (6)	−0.0008 (4)	0.0047 (5)	0.0027 (4)
C1	0.0205 (5)	0.0206 (6)	0.0186 (6)	0.0005 (5)	0.0066 (4)	0.0004 (5)
C10	0.0254 (6)	0.0225 (6)	0.0238 (6)	0.0012 (5)	0.0053 (5)	0.0000 (5)
C12	0.0364 (7)	0.0220 (6)	0.0263 (7)	0.0014 (5)	0.0140 (5)	0.0011 (5)
C6	0.0243 (6)	0.0275 (7)	0.0245 (6)	−0.0001 (5)	0.0063 (5)	0.0015 (5)
C14	0.0271 (7)	0.0198 (6)	0.0389 (8)	−0.0013 (5)	0.0068 (6)	−0.0056 (5)
C3	0.0218 (6)	0.0325 (7)	0.0272 (7)	−0.0019 (5)	0.0013 (5)	−0.0023 (5)
C9	0.0279 (7)	0.0290 (7)	0.0273 (7)	0.0057 (5)	−0.0004 (5)	−0.0023 (5)
C8	0.0193 (6)	0.0355 (8)	0.0363 (7)	0.0025 (5)	0.0031 (5)	−0.0088 (6)
C7	0.0237 (6)	0.0367 (8)	0.0332 (7)	−0.0033 (5)	0.0110 (5)	−0.0034 (6)
C2	0.0189 (6)	0.0346 (7)	0.0335 (7)	0.0017 (5)	0.0023 (5)	0.0002 (6)
C13	0.0314 (7)	0.0198 (6)	0.0415 (8)	0.0014 (5)	0.0148 (6)	0.0041 (5)

Geometric parameters (Å, º)

S1—C1	1.8125 (12)	C12—C13	1.4295 (18)
S1—C2	1.7992 (14)	C6—H6	0.9500
O2—C4	1.2308 (15)	C6—C7	1.3874 (18)
O1—C11	1.3687 (14)	C14—H14	0.9500
O1—C14	1.3779 (16)	C14—C13	1.333 (2)
N1—C5	1.4505 (15)	C3—H3A	0.9900
N1—C4	1.3621 (15)	C3—H3B	0.9900
N1—C1	1.4765 (15)	C3—C2	1.5169 (19)
C11—C1	1.4954 (17)	C9—H9	0.9500
C11—C12	1.3448 (18)	C9—C8	1.385 (2)
C5—C10	1.3870 (17)	C8—H8	0.9500
C5—C6	1.3876 (18)	C8—C7	1.385 (2)
C4—C3	1.5188 (16)	C7—H7	0.9500
C1—H1	1.0000	C2—H2A	0.9900
C10—H10	0.9500	C2—H2B	0.9900
C10—C9	1.3935 (18)	C13—H13	0.9500
C12—H12	0.9500		
C2—S1—C1	95.20 (6)	C7—C6—H6	120.2
C11—O1—C14	106.07 (10)	O1—C14—H14	124.7
C5—N1—C1	114.93 (9)	C13—C14—O1	110.60 (11)
C4—N1—C5	119.22 (10)	C13—C14—H14	124.7
C4—N1—C1	125.08 (10)	C4—C3—H3A	107.7
O1—C11—C1	116.58 (10)	C4—C3—H3B	107.7
C12—C11—O1	110.14 (11)	H3A—C3—H3B	107.1
C12—C11—C1	133.28 (11)	C2—C3—C4	118.65 (11)
C10—C5—N1	119.18 (11)	C2—C3—H3A	107.7
C10—C5—C6	120.58 (11)	C2—C3—H3B	107.7
C6—C5—N1	120.21 (11)	C10—C9—H9	119.9
O2—C4—N1	120.88 (11)	C8—C9—C10	120.13 (12)
O2—C4—C3	118.05 (11)	C8—C9—H9	119.9
N1—C4—C3	121.01 (11)	C9—C8—H8	119.9
S1—C1—H1	107.2	C9—C8—C7	120.17 (12)
N1—C1—S1	113.03 (8)	C7—C8—H8	119.9
N1—C1—C11	109.10 (9)	C6—C7—H7	120.0
N1—C1—H1	107.2	C8—C7—C6	120.09 (13)
C11—C1—S1	112.71 (8)	C8—C7—H7	120.0
C11—C1—H1	107.2	S1—C2—H2A	109.7
C5—C10—H10	120.3	S1—C2—H2B	109.7
C5—C10—C9	119.36 (12)	C3—C2—S1	109.81 (9)
C9—C10—H10	120.3	C3—C2—H2A	109.7
C11—C12—H12	126.6	C3—C2—H2B	109.7
C11—C12—C13	106.73 (12)	H2A—C2—H2B	108.2
C13—C12—H12	126.6	C12—C13—H13	126.8
C5—C6—H6	120.2	C14—C13—C12	106.46 (12)
C5—C6—C7	119.67 (12)	C14—C13—H13	126.8

O2—C4—C3—C2	−167.11 (12)	C4—N1—C1—C11	−92.17 (13)
O1—C11—C1—S1	77.57 (11)	C4—C3—C2—S1	−47.73 (15)
O1—C11—C1—N1	−156.00 (9)	C1—S1—C2—C3	61.81 (10)
O1—C11—C12—C13	0.57 (15)	C1—N1—C5—C10	64.62 (14)
O1—C14—C13—C12	−0.11 (16)	C1—N1—C5—C6	−113.03 (12)
N1—C5—C10—C9	−178.37 (11)	C1—N1—C4—O2	174.61 (11)
N1—C5—C6—C7	178.32 (11)	C1—N1—C4—C3	−8.21 (17)
N1—C4—C3—C2	15.63 (18)	C1—C11—C12—C13	−178.65 (13)
C11—O1—C14—C13	0.45 (14)	C10—C5—C6—C7	0.71 (19)
C11—C12—C13—C14	−0.28 (16)	C10—C9—C8—C7	0.4 (2)
C5—N1—C4—O2	5.23 (17)	C12—C11—C1—S1	−103.25 (15)
C5—N1—C4—C3	−177.59 (11)	C12—C11—C1—N1	23.17 (18)
C5—N1—C1—S1	−156.14 (8)	C6—C5—C10—C9	−0.74 (19)
C5—N1—C1—C11	77.62 (12)	C14—O1—C11—C1	178.73 (10)
C5—C10—C9—C8	0.2 (2)	C14—O1—C11—C12	−0.63 (13)
C5—C6—C7—C8	−0.1 (2)	C9—C8—C7—C6	−0.4 (2)
C4—N1—C5—C10	−124.95 (12)	C2—S1—C1—N1	−55.69 (9)
C4—N1—C5—C6	57.40 (16)	C2—S1—C1—C11	68.60 (9)
C4—N1—C1—S1	34.08 (14)		

Hydrogen-bond geometry (Å, º)

D—H···*A*	*D*—H	H···*A*	*D*···*A*	*D*—H···*A*
C10—H10···O2^{i}	0.95	2.54	3.4276 (16)	155
C12—H12···O1^{ii}	0.95	2.58	3.4583 (16)	153
C14—H14···O2^{iii}	0.95	2.50	3.4252 (16)	166
C13—H13···O2^{iv}	0.95	2.43	3.3641 (16)	168

Symmetry codes: (i) *x*, −*y*+1/2, *z*+1/2; (ii) *x*, −*y*+3/2, *z*−1/2; (iii) *x*, −*y*+3/2, *z*+1/2; (iv) *x*, *y*+1, *z*.